

Coke deposition and product distribution in the co-cracking of waste polyolefin derived streams and vacuum gas oil under FCC unit conditions

Elena Rodríguez, Gorka Elordi, José Valecillos, Sepideh Izaddoust, Javier Bilbao, José M. Arandes, Pedro Castaño*

Chemical Engineering Department, University of the Basque Country UPV/EHU, P.O. Box 644-48080, Bilbao, Spain

Abstract

The effect of co-cracking of high-density polyethylene (HDPE) or its pyrolysis wax together with vacuum gasoil (VGO) has been studied. The aim is determining the content, nature and location of coke while analyzing the impact on product distribution in the process. Four different feeds were used (VGO, VGO + 5 wt% HDPE, VGO + 20 wt% of wax and 100 wt% wax) in experiments performed in a laboratory-scaled riser simulator, with similar conditions than these of the fluid catalytic cracking (FCC) unit: equilibrated catalyst; 530 °C; catalyst/feed mass ratio, 5; contact time, 6 s. The results of the different characterization techniques of the deactivated catalyst and the coke indicate that the catalyst fouling decreases notably by incorporating these waste streams, changing its nature to a more aliphatic (olefinic) one and its location toward the zeolite micropores. On the contrary, the coke formed from the VGO is more evolved and mainly constituted by polyaromatic components deposited on the mesopores of the catalyst matrix. Product distribution is also affected, increasing the yield of light cycle oil and keeping a relatively similar gasoline yield, with greater olefinity and lower aromaticity. Thus, the FCC shows great perspectives to valorize polyolefins, present in waste plastics, at great scale.

Keywords: polyolefin recycling; waste valorization; cracking; FCC; deactivation; coke

1. Introduction

The interest in plastic recycling is justified by its growing production and consumption. Particularly due to the environmental problems related with their inappropriate management as waste within the municipal solid waste (MSW). In fact, dumped plastics have reached unacceptable limits within the marine environment [1]. In this framework, the refining industry has the suitable infrastructure to transform back the urban and industrial hydrocarbon wastes (plastics or tires) into commodities such as light olefins, aromatics or gasoline. In particular, the fluid catalytic cracking (FCC) unit has a great versatility to process such complex feeds with the more standard one such as vacuum gas oil (VGO). Analogous and important works proving this hypothesis about the FCC unit capacity are these dealing with the co-cracking of atmospheric or vacuum residue [2,3], recycling cuts [4,5], light crude oil [6] and biomass derived feedstock like bio-oil [7–10].

A group from the Indian Institute of Technology Delhi made an important contribution to the joint valorization of waste plastics and secondary interest refinery streams. They carried out a thermal co-cracking of plastics with refinery streams (petroleum vacuum residue, VR), and different biomass and coal sources with a N₂ stream. Thus, they fed binary, ternary and quaternary feeds. The thermogravimetric [11–13] and batch [14,15] reactor results show the existence of significant synergies due to the reactions among the reaction intermediates as the activation energy decreases compared to those corresponding to the individual components. Hence, improvements are obtained in the yields and compositions of the liquid products. The co-cracking of high-density polyethylene (HDPE) together with VR gives way to a high liquid yield (56 wt% at 550 °C) with an aliphatic content of 89.9 wt%. The components of this liquid mainly correspond to the diesel fraction, and 22 wt% to the gasoline fraction [16]. These authors [17] have also studied the use of different catalysts in the co-cracking of binary and tertiary mixtures of VR, jatropha oil, and HDPE. The higher reaction rate compared to the thermal cracking stands out. Thus, in the co-cracking of VR and HDPE with an HZSM-5 catalyst operating at 450 °C, an 83 wt% of liquid yield is obtained (34 wt% in the non-catalytic reaction) with a gasoline range hydrocarbons of 8 wt% and 71 wt% of diesel compounds. The content of olefins accounts for 45 wt%, whereas there were none in the non-catalytic process, which is due to the catalytic cracking of the HDPE that was fed.

The main findings in the use of FCC unit to valorize waste plastics are aligned with the cracking of polyolefins, which are the majoritarian fraction within the MSW. The pioneering work of Ng [18] pointed to the high yield of gasoline from the co-cracking of high-density polyethylene

(HDPE, 10 wt%) and VGO, in a micro-activity test (MAT) reactor at 510 °C. Further works, using different catalysts such as commercial and laboratory-made with HY and/or HZSM-5 zeolites, targeted several different alternatives: (i) co-cracking of polyolefins directly dissolved into the VGO or light cycle oil (LCO) [19–23], or (ii) the co-cracking of polyolefin pyrolysis product (waxes) [24–26]. The second route is considered more interesting because it offers the advantage that the pyrolysis can be carried out in a delocalized way using small facilities located at waste plastic collection and classification points [27,28]. Moreover, the composition of the waxes, in addition to their fusion point (~70 °C), density, and viscosity, are adequate as FCC co-feedstock [29].

In the design of the FCC unit, the properties of the catalyst are conditioned by the product distribution and the lessening of catalyst deactivation for a given feedstock. These conditionings also apply to the overall design of the unit, which has a fluidized reactor with vertical transportation of both the catalyst and feed/products, namely the riser, a stripper and a fluidized bed regenerator [30,31]. The cracking catalysts are based on HY zeolite crystals embedded in a matrix with meso- and macropores made out of alumina, clays, and other additives [32]. The matrix provides different functionalities [33,34]: (i) resistance against catalyst attrition, (ii) certain catalytic activity for the bulkiest molecules (which cannot penetrate in the zeolite micropores), (iii) retain metals such as V, Ni or Fe [35,36] and (iv) attenuate the pore blocking of the zeolite by coke.

The reaction network in the cracking section (riser) is complex due to the massive number of reactions occurring simultaneously: β -scission, isomerization, hydrogen transfer, cyclation, aromatization and coke formation, among others [37–39]. As a consequence of the partial blockage of the acid sites of the zeolite by coke, the catalyst is deactivated within the limited contact time between the catalyst and the feed (in the order of seconds). This used catalyst circulates to the stripper and the regenerator to recover its activity [40]. The efficiency of coke removal by the regenerator, together with the intrinsic nature and location of the coke formed, have a notable effect on the product distribution and overall efficiency of the unit [41].

Cerqueira et al. [42] have studied the complex composition of the coke deposited under industrial FCC conditions using multiple techniques. This work led to a comprehensive review on the topic [43]. These authors and others [44–47] have examined the impact of catalyst and feed properties on the mechanisms of coke formation, placing a great deal of significance on its origin (catalytic and thermal coke) and its location on the catalyst surface (inside the micropores or on the matrix mesopores).

In this work, we have studied the impact of co-feeding HDPE or HDPE derived pyrolysis wax with vacuum gasoil (VGO) on product distribution and, in more detail, on coke formation. Four different alternative feeds were used in particular: vacuum gasoil (VGO), VGO mixed with 5 wt% of high-density polyethylene (HDPE), VGO mixed with 20 wt% of wax from the pyrolysis of HDPE, and that wax alone. The selection of 20 wt% of waxes in the feed mixture is justified because of the large capacity of the FCC units, and thus the interest of a larger fraction is not considered. The 5 wt% of HDPE is motivated by the experimental difficulties of feeding a more concentrated solution into the reactor. The feed of pure VGO and waxes has the goal of comparing the results with a common refinery feed and those of the co-cracking, respectively. The feeds have been characterized and then cracked in a mini-fluidized CREC reactor, using an equilibrated industrial FCC catalyst. This reactor enables to mimic the industrial FCC conditions faithfully[48–51]. The properties of the used catalyst as well as the content, nature, and location of coke have been studied by several analytical techniques: N₂ adsorption-desorption; temperature programmed oxidation (TPO); Fourier Transformed infrared (FTIR) spectroscopy; TPO-MS (mass spectrometry) coupled with FTIR spectroscopy; Raman spectroscopy, and laser desorption ionization time-of-flight mass spec (LDI TOF-MS). The features of the coke have been correlated with those of the feed in order to establish its implications within the co-cracking of alternative residual streams as feed for the FCC unit.

2. Experimental

2.1. Feeds

The vacuum gas oil (VGO) was supplied by Petronor S.A. (Muskiz, Spain) and it is a representative and standard FCC feed. The high-density polyethylene (HDPE) was supplied by Dow Chemical (Tarragona, Spain) as 4 mm diameter pellets. The wax was obtained by fast pyrolysis of HDPE in a conical spouted bed reactor at 500 °C in a pilot-plant [29]. The blends have been obtained by mixing 5 wt% HDPE or 20 wt% of wax in VGO.

The composition of the feeds was determined by simulated distillation in an Agilent 6890 Series GC gas chromatograph, according to the ASTM D-2887 standard. The simulated distillation of the wax was carried out diluting this feed by half its mass of tetrahydrofuran (THF) at 55 °C. Additional compositional information of the feeds was obtained in a bi-dimensional Agilent 7890A gas chromatograph (GC×GC) provided with two columns and a flow modulator,

coupled in line with an Agilent 5975C Series mass spectrometer (MS) and a flame ionization detector (FID) [52].

The thermal behaviors of HDPE and wax were analyzed by thermogravimetric analysis (TGA) in a Q5000-IR of TA Instruments, with a N₂ flow-rate of 32 cm³ (N) min⁻¹ and a heating rate of 10 °C min⁻¹ from ambient temperature to 700 °C. The density of the feeds was calculated according to ASTM D4052 standard. The API gravity was calculated according to the ASTM D287 standard and following the procedure 2B2.3 of the API technical data book. The average molecular weight was computed from the kinematic viscosity, which was obtained following the 2B2.3 procedure of the API technical data book. The high heating value (HHV) was determined by differential scanning calorimetry (DSC), with a Setaram TG-DSC 111 calorimeter. The experimental procedure consists of the combustion of the feed with air following a 5 °C min⁻¹ heating rate from 20 to 750 °C.

2.2. Reaction equipment

The reaction unit is an FCC riser simulator, designed and assembled by the chemical reaction engineering center (CREC) in London (ON, Canada), mimics the industrial condition at laboratory scale [48–51]. The reactor (Figure 1) consists of a catalyst basket bounded by two grids trapping the catalyst and restraining the catalyst mobility within this chamber. The assumption of well-mixed conditions in the reactor can be supported by the high gas recirculation rate due to the rotation of an impeller positioned above the catalyst basket. Once the preset reaction time (of the same order as the contact time in the riser reactor) has been completed, the reactor and vacuum box are connected, and a sample of product is sent to a chromatographic device. The reaction conditions were as follows: 530 °C (the fluidized bed regime ensures isothermicity); reaction time, 6 s (once reaction time has elapsed the products are extracted by vacuum, avoiding side reactions); catalyst/feed mass ratio on a dry basis, 5 g_{catalyst} (g_{feed})⁻¹. The product stream was analyzed online with a gas chromatograph (Agilent Technologies 7890 A, with FID and PFPD detectors) equipped with an HP-PONA Column (Agilent Technologies, 50 m long, 0.2 mm internal diameter and 0.5 μm in thickness). The analysis starts at -30 °C (3 min) to ensure a proper separation of the lightest fractions and continues with a 15 °C min⁻¹ ramp until 235 °C, keeping it for 1 min and increasing the temperature up to 320 °C with a 30 °C min⁻¹ ramp to extract the heaviest compounds. Identification of the species was carried out in a GC-MS spectrometer (Shimadzu QP2010) comparing the data obtained from the spectra with the NIST library data. A similarity higher than 95% was required in order to assign the peak with the suggested component. The products

have been grouped into lumps: dry gas (C₁–C₂), liquefied petroleum gases (LPG, C₃–C₄), gasoline (C₅–C₁₂, corresponding approximately to the limit boiling point, BP < 216 °C), light cycle oil (LCO, C₁₃–C₂₀), heavy cycle oil (HCO, C₂₀₊), and coke. The amount of coke was assessed by combustion in a TGA (Q5000 de TA Instruments), with a heating rate of 3 °C min⁻¹ from 300 to 550 °C.

The conversion was defined as in the catalytic cracking of commercial feedstock, that is, as the sum of the following reaction product lumps: dry gas (C₁–C₂), liquefied petroleum gases (LPG, C₃–C₄), and gasoline (C₅–C₁₂). Hence, light cycle oil (LCO, C₁₃–C₂₀) and heavy cycle oil (HCO, C₂₀₊), which are the main feedstock for the FCC unit, were not considered. The yield has been defined as the ratio (in mass percentage) of each fraction related to the total mass fed.

$$Yield_i = \frac{\text{mass of fraction}_i}{\text{mass of feed}} \cdot 100 \quad (1)$$

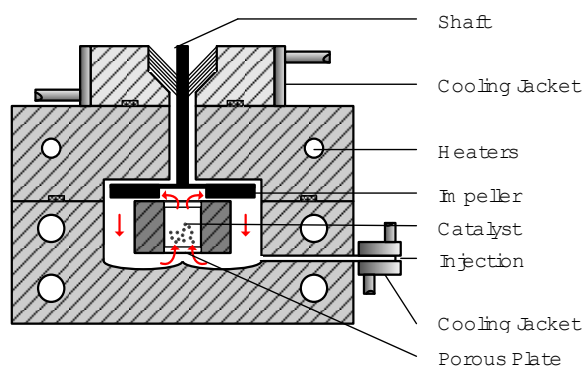


Figure 1. Scheme of riser simulator reactor [48].

2.3. Fresh and used catalyst characterization

A commercial FCC equilibrium catalyst (used in refinery) containing 15 wt% of HY zeolite was used. The physical properties of the catalyst (surface area, pore volume, and distribution) were determined by N₂ adsorption-desorption at -196 °C (Micromeritics ASAP 2010), using the BET and BJH methods, respectively. Samples were previously outgassed for 8 h at 150 °C under vacuum. The crystal structure was determined by X-ray diffraction (Philips X'PERT PRO diffractometer operating at 40 kV and 40 mA in theta-theta configuration with a secondary monochromator with CuKα1 radiation at a wavenumber of 1.5418 Å. An energy dispersive PIXcel detector was used with an active length of 2q = 3.347 Å. The acidity was obtained by temperature-programmed desorption (TPD) of previously absorbed NH₃ (at 150 °C) by means of a mass spectrometer (Balzers Instruments Thermostar) connected on-line to a calorimeter

Setaram TG-DSC 111) following a ramp of 5 °C min⁻¹ to 550 °C. The Brönsted/Lewis (B/L) acid site ratio has been determined by analyzing the region of 1400–1700 cm⁻¹ in the FTIR spectrum of adsorbed pyridine, which has been obtained using a Specac catalytic chamber connected on-line with a Nicolet 6700 FTIR spectrometer. The results have been determined from the ratio between the intensity of pyridine adsorption bands at 1545 and 1450 cm⁻¹ and taking into account the molar extinction coefficients of both adsorption bands ($\epsilon_B = 1.67 \text{ cm } \mu\text{mol}^{-1}$ and $\epsilon_L = 2.22 \text{ cm } \mu\text{mol}^{-1}$).

The physical properties of the catalyst used are summarized in Table 1, whereas the NH₃ TPD and pyridine adsorption FTIR analysis results are shown in Figure 2. The physical properties of the catalyst displayed in Table 1, are typical for an equilibrium FCC catalyst. The NH₃ TPD showed two peaks (Figure 2a), related to two types of weak acid sites located at 240 and 282 °C [53,54]. The intensity of the first peak is about 2.5 times larger than that of the second one. This weak acidity distribution is also in accordance with an equilibrium FCC catalyst that had undergone several reaction/regeneration cycles and suffered partial dealumination [55,56]. The BAS/LAS sites ratio, the relationship between the absorbance intensity of 1545 and 1445 cm⁻¹ FTIR bands multiplied by each molar extinction coefficient, is of 1.12 (Figure 2b). Once more, this low ratio compared with a freshly synthesized zeolite is standard for FCC catalysts [57].

The physical properties of the used catalysts and the location of coke were determined by N₂ adsorption–desorption (Micromeritics ASAP 2010) using the same methodology described before. The amount, nature-location of coke deposited in the catalyst has been determined by temperature programmed oxidation (TPO) with air in a TGA SDT 2960 from TA Instruments, following a ramp of 3 °C min⁻¹ from 300 to 550 °C. Samples (3-5 mg) have been swept for 3 h with a He flow at 550 °C prior to the analysis to remove volatile coke species and thereby reproduce the performance of the stripping section of the unit [58]. The FTIR and FTIR-TPO spectra were obtained in a Nicolet 6700 (Thermo) using a transmission cell, 60 scans, and a resolution of 4 cm⁻¹. The samples of catalysts (3–5 mg) were pelletized with KBr (300 mg, purity > 99%), applying pressures equivalent to 10 t cm⁻² for 10 min. In the case of FTIR-TPO the samples were first degassed at 100 °C under vacuum and then subjected to a linear temperature program (up to 550 °C, 5 °C min⁻¹) under 60 mL min⁻¹ of air, recording FTIR spectra at a frequency of 12 h⁻¹. Simultaneously, the signal of CO₂ (m/z = 44) was recorded on a mass spectrometer OmniStar ThermoStar GDS 320 Pfeiffer Vacuum. This methodology have proved to be useful to characterize several aspect of coke [59]. Raman spectroscopy was performed in a Renishaw confocal microscope using two excitation beams of 514 nm

wavelength, and subtracting the fluorescence caused by coke. The measurements were taken over 3–5 mg of catalyst, performing at least 3 analyses at different positions and reducing the exposure to air for avoiding coke oxidation. The laser desorption-ionization (LDI) coupled with a time of flight mass spectrometer (TOF MS) spectrometer allows for measuring molecular weights of large organic molecules like the polyaromatics of coke that are easily fragmented by other more conventional techniques [60]. The analysis was carried out in a Bruker Autoflex Speed unit equipped with an Nd-YAG laser of 355 nm that applies short pulses at high vacuum conditions.

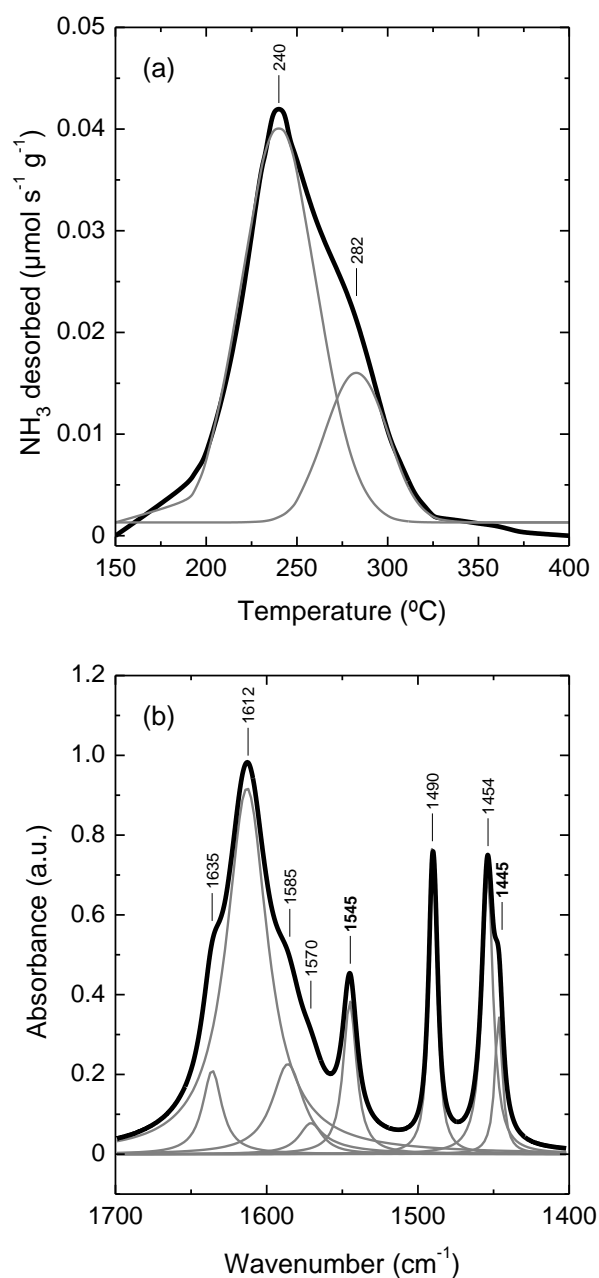


Figure 2. NH₃ TPD analysis (a) and FTIR spectrum of pyridine adsorbed (b) of the fresh catalyst.

Table 1. Physical properties of the commercial catalyst used.

BET surface area (m ² g ⁻¹)	124.0
Micropore area (m ² g ⁻¹)	87.4
Mesopore area (m ² g ⁻¹)	36.6
Zeolite content (wt%)	13.8
Micropore volume (cm ³ g ⁻¹)	0.04
Unit cell size (Å)	24.26
Bed density (g cm ⁻³)	0.90
Mean particle diameter (µm)	55
Particle size distribution:	
< 40 µm (wt%)	0
< 80 µm (wt%)	67
< 105 µm (wt%)	87
< 149 µm (wt%)	99

3. Results

3.1. Properties of the feeds

Figure 3 shows the main BP fractions in the feeds (Figure 3a) and the main chemical fractions (Figure 3b) in terms of paraffins (P), isoparaffins (I), olefins (O), naphthenes (N), and aromatics (A). Figure 3a have been obtained by simulated distillation and Figure 3b have been obtained by GC×GC analysis. VGO contains two main BP fractions within the region of 321-425 and 425-510 °C, corresponding to light and heavy vacuum gasoils, respectively. At the same time, the VGO shows much lower concentration of in the regions 271-321, 510-564 and > 564 °C.

Figure 3b shows that the main chemical fraction in VGO is the aromatic one, followed by aliphatics. On the other hand, the wax shows a very broad distribution of BP fractions centered in light vacuum gasoil and high concentrations of heavy vacuum gasoil and residue. Besides, this feed is a mixture of olefins, paraffins and isoparaffins. The composition of VGO+wax blend could be anticipated with the compositions of its individual constituents, and that of VGO+HDPE bears more resemblance to VGO with a certain amount of heavier species.

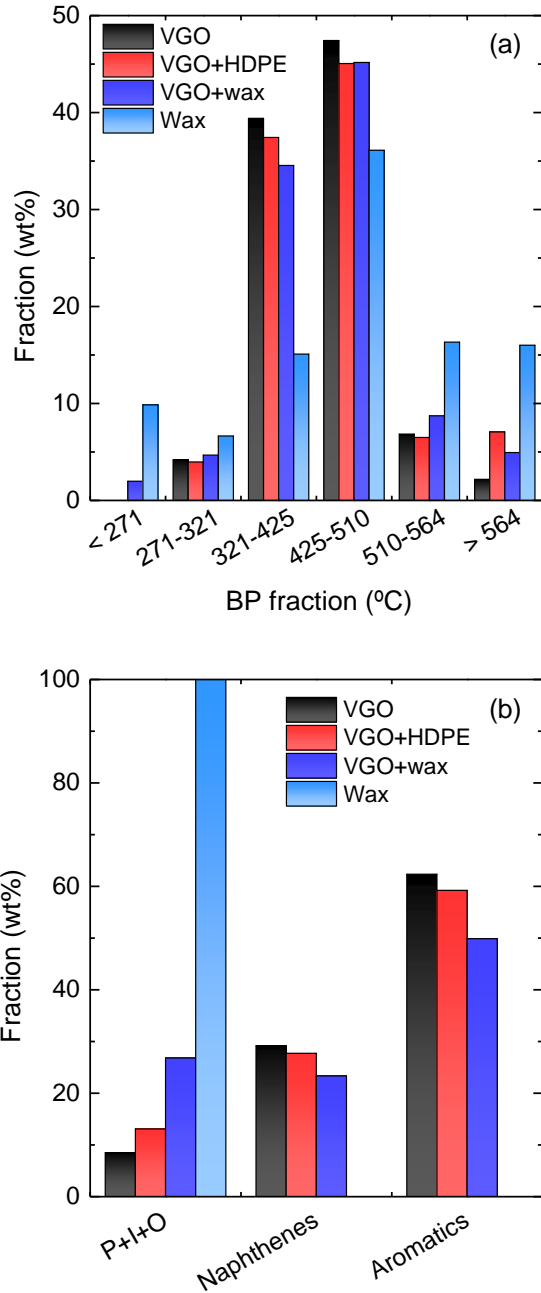


Figure 3. Simulated distillation results (a) and GCxGC analysis results (b) of the different feeds used.

The thermal behavior of HDPE and its wax is represented in Figure 4. The volatilization of HDPE can be ascribed to the solely pyrolysis of the material, which occurs at ~470 °C. The volatilization of the wax can be ascribed to two sequenced processes, evaporation of the lightest fraction (proved to be present in Figure 3) and pyrolysis of the heaviest fraction at ~460 °C, relatively similar to that pyrolysis temperature of HDPE.

All three feeds in Table 2 showed a similar density ($\sim 930 \text{ kg m}^{-3}$) and HHV ($\sim 43 \text{ MJ kg}^{-1}$), that is, wax could be treated in a FCC unit in a similar way to VGO and the energy balance would not be compromised either. Handling of VGO and wax in the installation would also be comparable according to their similar API gravity values. The main difference among the feeds consists of their mean molecular weight, the VGO being the lightest, 405 g mol^{-1} , wax with an intermediate value, 1430 g mol^{-1} , and the HDPE is by far the heaviest, $46,200 \text{ g mol}^{-1}$. The latter is due to the long linear paraffinic chains of the HDPE, in comparison to the shorter chains of wax and the much more aromatic nature of the VGO.

Table 2. Physical properties of the materials used.

	VGO	HDPE	Wax
Density at 15°C (kg L^{-1})	0.93	0.94	0.93
API gravity ($^{\circ}\text{API}$)	21.1		20.6
M_w (g mol^{-1})	405.3	46,200	1,430
HHV (MJ kg^{-1})	42	43	44

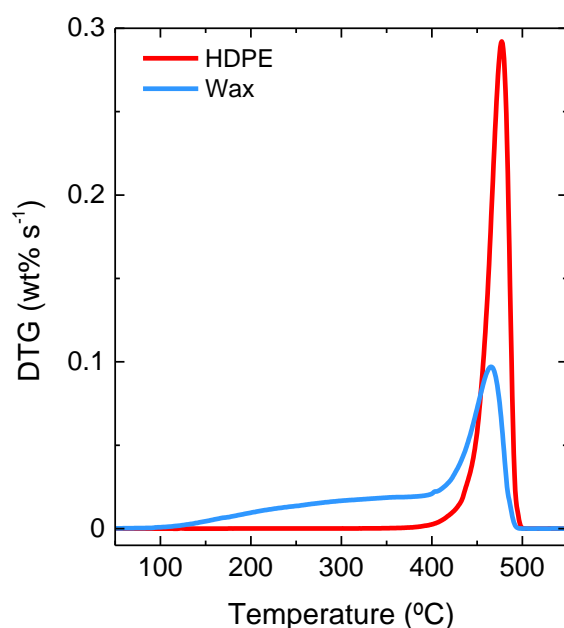


Figure 4. TGA analysis of the HDPE and waxes produced in its pyrolysis.

3.2. Conversion and yields

The conversions obtained, calculated as the summation of product yields (light gases, LPG, gasoline, and coke), were very similar in all cases: 53, 53, 52 and 50 wt% for VGO, VGO+HDPE, VGO+wax and wax, respectively. The smaller conversion of wax is due to the

fact that this feed is the heaviest (Figure 3a) although it is relatively “reactive” due to the higher content of olefins, paraffins, and isoparaffins (Figure 3b). As is observed in Figure 5a, where the product distributions for the four feeds are shown, the yields of dry gas, LPG, and gasoline are very similar in all cases but that of LCO is much higher for wax compared to the rest (43 wt% compared to less than 30 wt%), whereas the yield of HCO is much lower (7.3 wt% compared to >17 wt%). This result is qualitatively the same as incorporating atmospheric residue [3].

Therefore, although a slightly lower conversion was obtained for the wax, the product distribution obtained is considerably lighter. A very important factor is that the yield of coke decreases -33% when wax is treated. The effect of the co-cracking on the content, nature, and location of coke has been studied in the following sections.

Figure 5b shows the distribution of the molecular families within the gasoline fraction obtained for each feed. The gasoline fraction obtained from VGO cracking contains the highest amounts of aromatics and isoparaffins, both being interesting for a high-octane number, even though the aromatics are restricted by environmental legislations. All the other alternatives with increasing amounts of HDPE derived fractions showed a noticeable decrease in the aromatics, the olefins being the lump that increases in the highest amount. The yields of naphthenes and isoparaffins decreased as well, while linear paraffins increased when wax was treated alone or when HDPE was dissolved in VGO. The dilution of wax in VGO did not involve a significant increase in olefins and linear paraffins. The weight fraction of isoparaffins remained constant instead when compared to VGO. This is a remarkable result as the dilution of wax in VGO leads to a decrease in aromatics while keeping the fraction of isoparaffins and not increasing that of olefins in high amount. All three effects are especially sought in order to fulfill commercial gasoline standards. The synergetic effect of the thermal co-cracking of HDPE and an oil derived stream (VR) has been previously established in the literature [15,16]. A decrease in aromatic components and an increase in aliphatic ones in the liquid products compared to the mean of individual cracking of the feeds was monitored. This result is attributed to the reaction intermediates of HDPE and VR cracking. The same authors [17] also observed an increase in the yield of liquid fraction and a more aliphatic nature of it in the co-cracking of HDPE and VR compared to the cracking of VR alone.

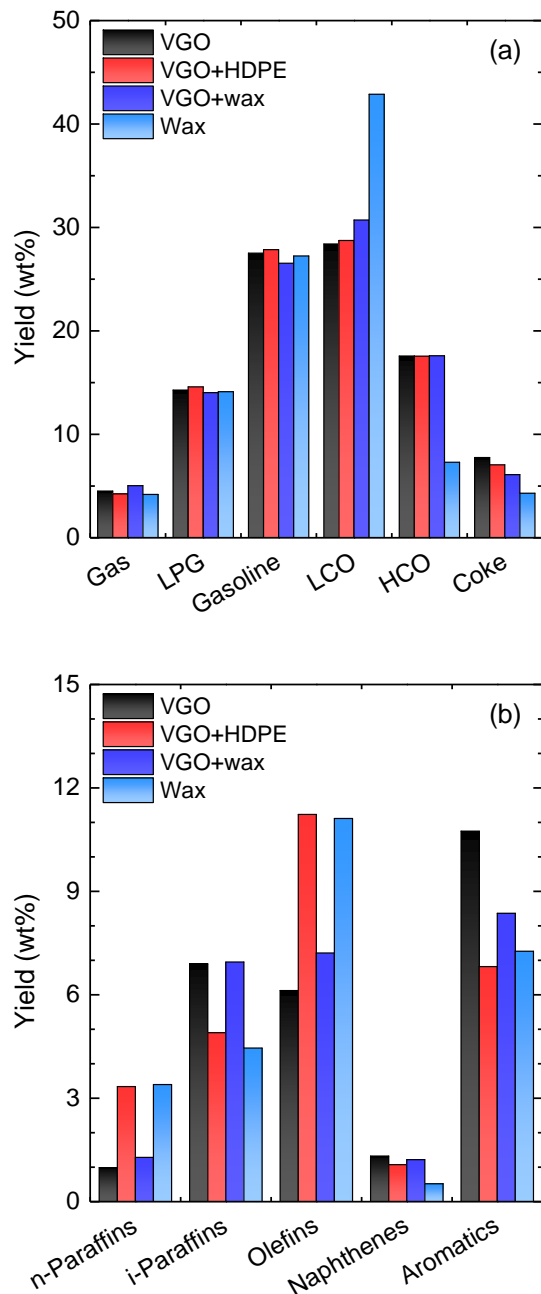


Figure 5. Fraction yields within the products (a) and molecular families within the gasoline fraction (b) for the different feeds used.

3.2. Location of coke

BET, meso- and micropore areas as well as average pore diameter of fresh and used catalysts are represented in Figure 6. All areas decrease after the reaction due to the presence of coke on the used catalysts. The fact that the average pore diameter increases indicates that coke is blocking more selectively the narrower pores of the catalysts. The degree of surface degradation

increases in the order $VGO < VGO+HDPE < VGO+wax < wax$, and the majority of this degradation is due to the decrease of micropore area. In fact, the mesopore area degradation is relatively similar regardless the type of feed used. These results combined indicate that the deposition of coke during VGO cracking occurs through “mesopore blockage”, decreasing the accessibility towards the micropores and the acid sites of the catalyst [43]. This effect is due to the matrix retention of species with two or more aromatic rings [61]. On the other hand, the coke formed during the cracking of HDPE or HDPE derived wax tends to degrade more the micropores, at the same degradation level of mesopores, indicating a higher degree of acid site blockage [62]. That is to say, cokes formed during the cracking of VGO are located towards the mesopores whereas the cokes formed during the cracking of HDPE derived streams are located towards the micropores of the catalyst.

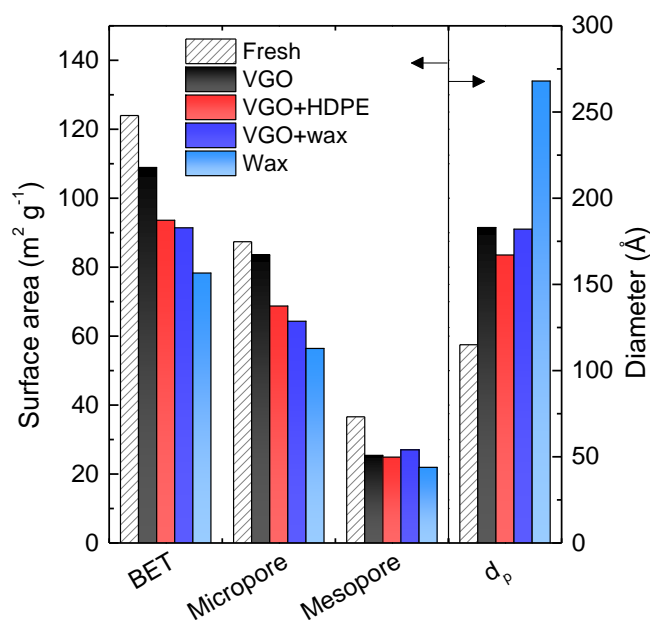


Figure 6. Physical properties: BET surface area, mesopore area, micropore area, and mean pore diameter of the used catalyst for the different feeds used.

3.3. Content and nature of coke

The TGA-TPO profiles of the coke deposited during the cracking of the different feeds used are shown in Figure 7. The area, position, and shape of the peaks indicates the amount of coke together with certain clues about its nature and location. The amount of coke present in the deactivated catalysts (referred to the mass of catalyst without coke) decreases in this order: VGO (1.55 wt%) > VGO+HDPE (1.41 wt%) > VGO+ wax (1.22 wt%) > wax (0.86 wt%). That

is, incorporation of wax can decrease the coke content on the catalyst up to -45%. The first and most important aspect of Figure 7, related with the yield of coke presented in Figure 5a, is that the amount of coke per catalyst mass lessens by the presence of HDPE derived streams. The temperature that corresponds to the maximum rate of weight loss follows the order: wax (530 °C) > VGO+HDPE (520 °C) > VGO+wax (515 °C) > VGO (505 °C). Assuming that the coke formed during the cracking of VGO is the most aromatic, this trend would support the previously explained fact displayed in Figure 6 that the coke deposited during VGO is placed in the mesopores and has a faster combustion rate (less limited by the diffusion) whereas the coke deposited during HDPE derived streams is placed in the micropores and has a slower combustion rate. However, an additional explanation of the different trends observed in Figure 7 could be related with a different composition of the cokes that, so far, cannot be neglected.

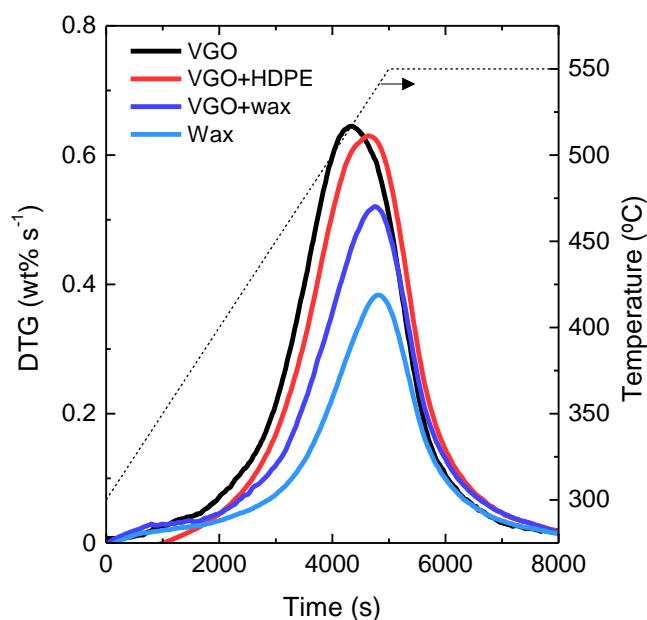


Figure 7. TG-TPO profiles of the used catalyst for the different feeds used.

To solve this, the composition of the coke has been assessed by FTIR spectroscopy. The main results of the 4 bands deconvolution of the FTIR spectra are shown in Figure 8. These bands are assigned to [63–68]: (i) C=C bonds of condensed aromatic structures at 1580 cm^{-1} , which also is known as “aromatic coke band”; (ii) conjugated C=C at 1610 cm^{-1} , which is known as “olefinic coke band”; (iii) C–H bonds in non-terminal aliphatic structures at 2922 cm^{-1} ; and (iv) C–H bonds in terminal aliphatic structures at 2960 cm^{-1} . The results presented in Figure 8 indicate that the nature of coke is a function of the feed in a way that the coke deposited during

VGO cracking is more aromatic and coke deposited during HDPE derived streams is more aliphatic (olefinic). This effect could be roughly anticipated from the compositions of the feed (Figure 3) and is nominally similar to the one occurring when the zeolite catalyst is modified by desilication [46]. And at the same time, they enable to indicate the combustion profile shown in Figure 7 can be directly linked with the location of coke (Figure 6). Otherwise, the coke deposited during the cracking of HDPE derived streams would eventually burn faster due to its higher aliphatic nature. The effect of the decrease in coke deposition, and the slowing down of its evolution towards condensed polyaromatic structures when the acidity of a catalyst is decreased, and/or when catalysts with no cages in pore intersections are used, is well established in the literature for biomass derived feedstocks catalytic conversion [67]. This coke evolution is also attenuated when the reaction temperature is decreased [66,69] and when the effective H/C ratio of the feed is increased [70]. In this paper, operating conditions of the FCC (high temperature, aromatic composition of the VGO, and cages in the pore intersections of the HY catalyst) favour the formation of coke and its evolution towards polyaromatic structures.

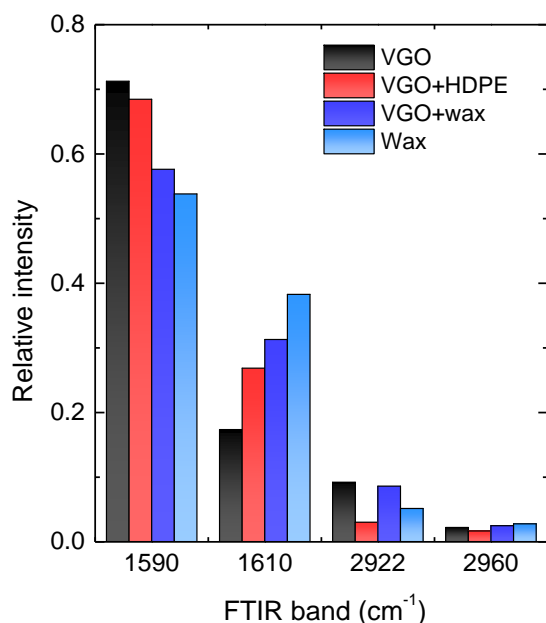


Figure 8. Relative intensities of four bands detected in the FTIR spectra of the used catalyst for the different feeds used.

Figure 9a shows the mass variation (CO_2 , $m/z = 44$) results in the coke combustion of the catalyst used for the cracking of different feeds. In Figure 9b-9e, the intensities of the four FTIR

characteristic bands of coke (1590, 1622, 2922, and 2960 cm^{-1}) are shown for the different feeds used. In Figure 9a, the presence of two peaks compared to the TGA-TPO is explained because of the lack of former sweeping. Thus, the first peak, the one that burns at low temperatures, corresponds to the combustion of the reaction medium species retained in the porous structure. The results have in common the evolution of the coke nature that takes place throughout the combustion, with a transformation (in the first combustion peak, $T < 400\text{ }^\circ\text{C}$, where light species are burned) in which an “aging” process of coke [57,71] takes place. In this “aging” process, C=C bonds that correspond to the aromatics (Figure 9b) and conjugated double bonds (Figure 9c) increase while those of aliphatics (C–H bonds of $-\text{CH}$, $-\text{CH}_2$, and $-\text{CH}_3$ at 2855-2955 cm^{-1}) decrease (Figures 9d and 9e) as they are either burned or transformed into a more condensed form of coke. This aging trend of coke through its combustion is observed for all the feeds. Later on, the combustion peaks of dienes and aromatics are similar (in relation to their amount) to all four used catalysts.

Raman spectra deconvolution results for the used catalysts used for the cracking of the different feeds are shown in Table 3. The Raman spectra of each used catalyst were deconvoluted in 5 significant bands: the $\nu_{\text{C-H}}$ band (1225 cm^{-1}), related to the vibration of C-H bonds, the D (1380 cm^{-1}) and D_2 (1616 cm^{-1}) bands that are related to the aromatic structure disorganization, the D_3 (1500 cm^{-1}) band that is related to structural imperfections of the aromatic clusters, and the G band (1595 cm^{-1}) related to the tangential elongation of the aromatic structures. The latter is considered as an index of the increase in order and thus, as an approximation to the graphite structure [9,63,72–75]. The ratio between the D and G band intensities ($I_{\text{D}}/I_{\text{G}}$) is related to the particle size of the coke. Although all values represent cokes that have evolved into polyaromatic structures (consequence of the severe conditions of the FCC unit), there are significant variations depending on the origin of the feed. Hence, the $I_{\text{C-H}}$ index order represents the aliphatic nature of the coke and it is in accordance with the results obtained in the FTIR analysis, that is: $\text{VGO} < \text{VGO+HDPE} < \text{VGO+ wax} < \text{wax}$. Similarly, the aromatic nature of the cokes (D band for the disorganized aromatic coke and G for the ordered grade of the coke) are also in congruence with the results obtained in the FTIR analysis for the PAHs band (opposite to the one observed for the aliphatics). Moreover, the $I_{\text{D}}/I_{\text{G}}$ ratio (related to the coke particle size) indicates that this size is larger for the deposited coke with a higher aromatic degree, as the coke is formed by polyaromatics whose size depends on their level of condensation.

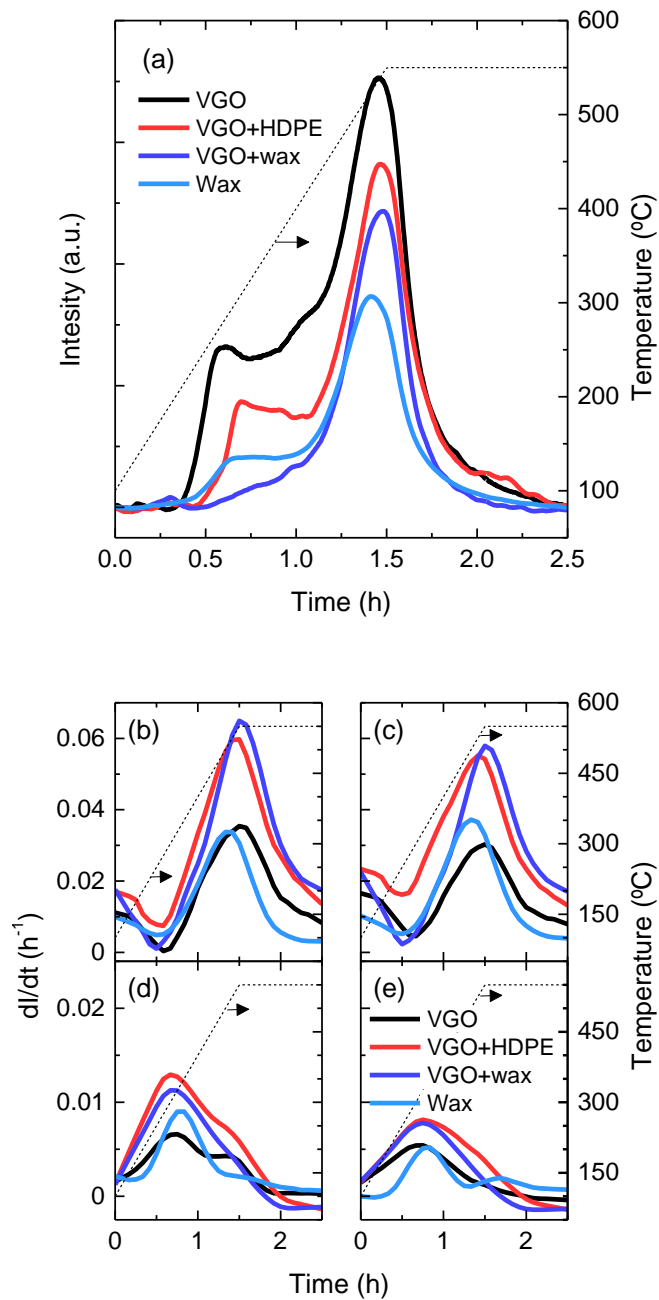


Figure 9. TPO profiles (a) and simultaneous profiles of the FTIR intensities of the bands at 1590 cm⁻¹ (b), 1622 cm⁻¹ (c), 2922 cm⁻¹ (d), and 2960 cm⁻¹ (e), corresponding to the used catalyst for the different feeds used.

Table 3. Relative intensity (I) of the characteristic Raman spectra of the used catalysts used with the different feeds.

	VGO	VGO+HDPE	VGO+wax	Wax
I _{C-H}	0.12	0.13	0.13	0.14
I _D	0.35	0.29	0.29	0.26
I _{D3}	0.06	0.08	0.07	0.05
I _G	0.35	0.30	0.31	0.29
I _{D2}	0.13	0.12	0.12	0.11
I _D /I _G	1.00	0.98	0.96	0.91

The LDI TOF-MS allows for measuring large organic molecules like those of coke that are easily fragmented by other more conventional techniques [76]. The molecular weight of polycondensed products present in the coke is estimated by this method. The analysis of the used catalysts showed (Figure 10) that the detected species were mostly the aromatics deposited on the catalyst matrix. Peaks are observed in three intervals: 100-150 Da, 250-450 Da and 550-700 Da, with differences of 1 Da between adjacent peaks. The first two peaks correspond to soluble and the last one to heavy and insoluble in dichloromethane coke fractions [77]. These results give an idea of the heterogeneity of the identified species. Nevertheless, the peaks are wider and more intense for the catalyst used in VGO cracking compared to those used in the cracking of VGO mixed with either HDPE or wax. These results show the more aromatic nature of the coke from the catalyst used for VGO cracking, which agrees with the results obtained previously with the other techniques. The considerable concentration of aromatics in the coke from the catalyst used for the cracking of wax is also noteworthy, but this result also confirms the results obtained by FTIR and Raman spectra. Moreover, several series separated by 14 Da are observed in all cokes, such as 328-342-356 Da. These series are associated with species that vary by a single $-\text{CH}_2-$ group. In general, these series follow a Gaussian distribution and recurrently appear as deactivating coke species [42,65,78].

The most intense signal masses are shown in Table 4, as well as a possible structure that explains them and the corresponding H/C ratio. It is worth mentioning that some of these aromatics were previously identified in the coke of used catalysts used in an FCC when wastes [42] and a VGO bio-oil mixture [65] were fed. These results were expected even if the feeds were different. Furthermore, some of the identified aromatics (those developed in lesser grade) were identified as well in the coke formed in an MTO process [78]. In this case, the origin of these species is related to the olefins present in the reaction medium. The structures proposed for molecular weights higher than 300 Da are based on coronene ($\text{C}_{24}\text{H}_{12}$), which can be

considered as an intermediate species that evolves into more condensed structures. The lightest significant peak (106 Da) is not noticeable in the coke of the catalyst used to treat VGO. On the other hand, species corresponding to 429, 457, 596, and 628 Da are not relevant in the catalyst used with wax.

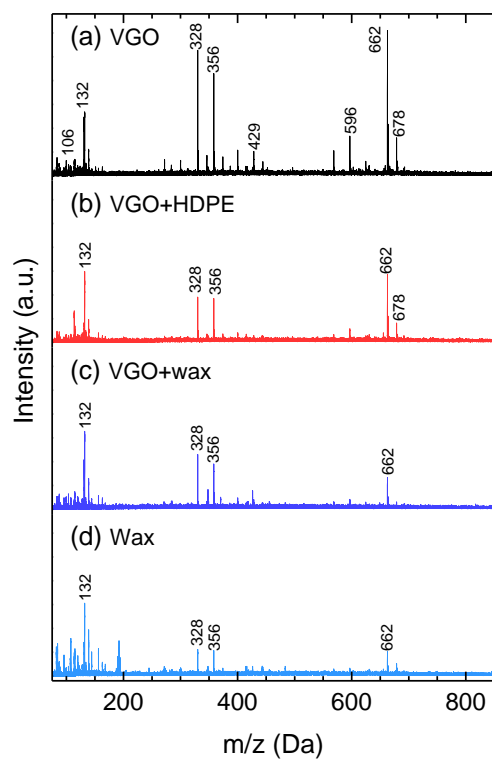
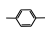
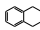
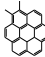
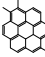
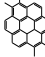
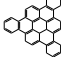
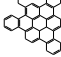
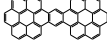
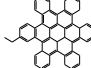
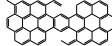
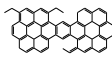


Figure 10. LDI TOF-MS spectra of the used catalyst for the different feeds used.

Table 4. Most intense coke structures of the used catalysts in the LDI MS-TOF spectra.

Mass (Da)	Formula	H/C	Structure
106	C ₈ H ₁₀	1.25	
132	C ₁₀ H ₁₂	1.20	
328	C ₂₆ H ₁₆	0.62	
342	C ₂₇ H ₁₈	0.67	
356	C ₂₈ H ₂₀	0.71	
429	C ₃₃ H ₃₃	1.00	
457	C ₃₅ H ₃₇	1.06	
596	C ₄₈ H ₂₀	0.42	
628	C ₅₀ H ₂₈	0.56	
662	C ₅₃ H ₂₆	0.49	
678	C ₅₄ H ₃₀	0.56	

4. Conclusions

The co-cracking of waxes derived from HDPE or dissolved HDPE in vacuum gas oil (VGO) do not affect the benchmark conversion of VGO, all in the range 49-53 wt%. The product distribution is not affected either, further than a slight increase of light cycle oil (LCO) yield with the HDPE derived streams. Incorporating plastic derived streams also has the positive outcome of enhancing the gasoline composition due to the decrease in aromatic content and the increase on that of olefins. Consequently, HDPE derived streams turn out to be potential and interesting co-feeds for the FCC unit.

It is important to indicate that the coke yield is significantly lessened with the co-cracking of HDPE derived streams. Besides, the results of the coke analysis by means of different techniques (FTIR spectroscopy, TPO-MS, Raman spectroscopy, and LDI TOF-MS) have shown that the nature and location of the coke is conditioned by the composition of the feed and by the hierarchical porous structure of the commercial FCC catalyst. Thus, the coke formed in the cracking of mixtures has a different nature to the one deposited on the cracking of VGO

alone, as it is less aromatic, more aliphatic and with the presence of long olefinic chains. These analyses of the coke and the N₂ absorption-desorption measurement of the used catalysts pore structure show that the formation of coke from HDPE and its pyrolysis waxes takes place in the micropores of the HY zeolite, whose shape selectivity limits the evolution towards condensed structures. On the other hand, the coke formed in the cracking of VGO (alone or in the mixtures) is constituted by polyaromatics formed from the condensation of the aromatic components of VGO and deposited on the mesopores of the catalyst matrix. These differences should be taken into account when establishing the best catalyst formulation to upgrade waste polyolefins in the FCC unit.

To sum up, the results presented in this work indicate that the FCC unit has outstanding properties to treat waste polyolefins on a great scale. Its versatility enables tuning the reaction conditions and the catalyst formulation in order to optimize this valorization even further. In these terms, waste polyolefin streams can be used to balance out the drawback of using more refractory gasoils (with severe coke fouling) to quench deactivation and increase the yield of middle distillates.

Acknowledgments

This research was funded by the Ministry of Economy and Competitiveness (MINECO) of the Spanish Government (CTQ2015-67425R and CTQ2016-79646-P), the European Regional Development Funds (ERDF) and the Basque Government (IT748-13). Dr. Rodriguez is thankful to the University of the Basque Country UPV/EHU (Zabalduz Programme). S. Izaddoust is thankful to the MINECO for her grant BES-2017-080077.

Literature

- [1] W.C. Li, H.F. Tse, L. Fok, Plastic waste in the marine environment: A review of sources, occurrence and effects, *Sci. Total Environ.* 566–567 (2016) 333–349. doi:10.1016/J.SCITOTENV.2016.05.084.
- [2] A. Devard, G. de la Puente, U. Sedran, Laboratory evaluation of the impact of the addition of resid in FCC, *Fuel Process. Technol.* 90 (2009) 51–55. doi:10.1016/j.fuproc.2008.07.009.
- [3] J.R. García, M. Falco, U. Sedran, Intracrystalline mesoporosity over Y zeolites.

- Processing of VGO and resid-VGO mixtures in FCC, *Catal. Today*. 296 (2017) 247–253. doi:10.1016/j.cattod.2017.04.010.
- [4] M.L. Fernández, A. Lacalle, J. Bilbao, J.M. Arandes, G. de la Puente, U. Sedran, Recycling hydrocarbon cuts into FCC units, *Energy Fuels*. 16 (2002) 615–621. doi:10.1021/ef010184i.
- [5] F.J. Passamonti, G. de la Puente, U. Sedran, Reconversion of olefinic cuts from fluidized catalytic cracking naphthas, *Ind. Eng. Chem. Res.* 43 (2004) 1405–1410. doi:10.1021/ie030467t.
- [6] A. Usman, A. Aitani, S. Al-Khattaf, Catalytic cracking of light crude oil: Effect of feed mixing with liquid hydrocarbon fractions, *Energy Fuels*. 31 (2017) 12677–12684. doi:10.1021/acs.energyfuels.7b02324.
- [7] A. Corma, L. Sauvanaud, FCC testing at bench scale: New units, new processes, new feeds, *Catal. Today*. 218–219 (2013) 107–114. doi:10.1016/j.cattod.2013.03.038.
- [8] N. Thegarid, G. Fogassy, Y. Schuurman, C. Mirodatos, S. Stefanidis, E.F. Iliopoulou, K. Kalogiannis, A.A. Lappas, Second-generation biofuels by co-processing catalytic pyrolysis oil in FCC units, *Appl. Catal. B Environ.* 145 (2014) 161–166. doi:10.1016/j.apcatb.2013.01.019.
- [9] Á. Ibarra, E. Rodríguez, U. Sedran, J.M. Arandes, J. Bilbao, Synergy in the cracking of a blend of bio-oil and vacuum gasoil under fluid catalytic cracking conditions, *Ind. Eng. Chem. Res.* 55 (2016) 1872–1880. doi:10.1021/acs.iecr.5b04502.
- [10] S.D. Stefanidis, K.G. Kalogiannis, A.A. Lappas, Co-processing bio-oil in the refinery for drop-in biofuels via fluid catalytic cracking, *WIREs Energy Environ.* 7 (2018) e281. doi:10.1002/wene.281.
- [11] M. Ahmaruzzaman, D.K. Sharma, Non-isothermal kinetic studies on co-processing of vacuum residue, plastics, coal and petrocrop, *J. Anal. Appl. Pyrolysis*. 73 (2005) 263–275. doi:10.1016/J.JAAP.2004.11.035.
- [12] S. Biswas, D.K. Sharma, Synergistic co-processing/co-cracking of *Jatropha* oil, petroleum vacuum residue, and high density polyethylene, *J. Renew. Sustain. Energy*. 4 (2012) 043112. doi:10.1063/1.4737924.
- [13] S. Biswas, P. Mohanty, D.K. Sharma, Studies on synergism in the cracking and co-cracking of *Jatropha* oil, vacuum residue and high density polyethylene: Kinetic analysis,

- Fuel Process. Technol. 106 (2013) 673–683. doi:10.1016/J.FUPROC.2012.10.001.
- [14] M. Ahmaruzzaman, D.K. Sharma, Coprocessing of petroleum vacuum residue with plastics, coal, and biomass and its synergistic effects, *Energy Fuels*. 21 (2007) 891–897. doi:10.1021/ef060102w.
- [15] M. Ahmaruzzaman, D.K. Sharma, Characterization of liquid products from the co-cracking of ternary and quaternary mixture of petroleum vacuum residue, polypropylene, Samla coal and Calotropis Procera, *Fuel*. 87 (2008) 1967–1973. doi:10.1016/J.FUEL.2008.01.007.
- [16] S. Biswas, D.K. Sharma, Co-cracking of jatropha oil, vacuum residue and HDPE and characterization of liquid, gaseous and char products obtained, *J. Anal. Appl. Pyrolysis*. 101 (2013) 17–27. doi:10.1016/J.JAAP.2013.03.003.
- [17] S. Biswas, S. Majhi, P. Mohanty, K.K. Pant, D.K. Sharma, Effect of different catalyst on the co-cracking of Jatropha oil, vacuum residue and high density polyethylene, *Fuel*. 133 (2014) 96–105. doi:10.1016/J.FUEL.2014.04.082.
- [18] S.H. Ng, Conversion of polyethylene blended with VGO to transportation fuels by catalytic cracking, *Energy Fuels*. 9 (1995) 216–224. doi:10.1021/ef00050a003.
- [19] J.M. Arandes, I. Abajo, D. López-Valerio, I. Fernández, M.J. Azkoiti, M. Olazar, J. Bilbao, Transformation of several plastic wastes into fuels by catalytic cracking, *Ind. Eng. Chem. Res.* 36 (1997) 4523–4529. doi:10.1021/ie970096e.
- [20] J.M. Arandes, J. Ereña, J. Bilbao, D. Lopez-Valerio, G. De la Puente, Valorization of polyolefins dissolved in light cycle oil over HY zeolites under fluid catalytic cracking unit conditions, *Ind. Eng. Chem. Res.* 42 (2003) 3952–3961. doi:10.1021/ie020986g.
- [21] F.J. Passamonti, U. Sedran, Recycling of waste plastics into fuels. LDPE conversion in FCC, *Appl. Catal. B Environ.* 125 (2012) 499–506. doi:10.1016/J.APCATB.2012.06.020.
- [22] A.O. Odjo, A.N. García, A. Marcilla, Conversion of low density polyethylene into fuel through co-processing with vacuum gas oil in a fluid catalytic cracking riser reactor, *Fuel Process. Technol.* 113 (2013) 130–140. doi:10.1016/J.FUPROC.2013.03.008.
- [23] A. Marcilla, M. del R. Hernández, Á.N. García, Degradation of LDPE/VGO mixtures to fuels using a FCC equilibrium catalyst in a sand fluidized bed reactor, *Appl. Catal. A Gen.* 341 (2008) 181–191. doi:10.1016/j.apcata.2008.02.041.

- [24] J.M. Arandes, I. Torre, M.J. Azkoiti, P. Castaño, J. Bilbao, H. de Lasa, Effect of catalyst properties on the cracking of polypropylene pyrolysis waxes under FCC conditions, *Catal. Today*. 133 (2008) 413–419. doi:10.1016/j.cattod.2007.12.080.
- [25] J.M. Arandes, I. Torre, P. Castaño, M. Olazar, J. Bilbao, Catalytic cracking of waxes produced by the fast pyrolysis of polyolefins, *Energy Fuels*. 21 (2007) 561–569. doi:10.1021/ef060471s.
- [26] J.M. Arandes, M.J. Azkoiti, I. Torre, M. Olazar, P. Castaño, Effect of HZSM-5 catalyst addition on the cracking of polyolefin pyrolysis waxes under FCC conditions, *Chem. Eng. J.* 132 (2007) 17–26. doi:10.1016/j.cej.2007.01.012.
- [27] E. Butler, G. Devlin, K. McDonnell, Waste polyolefins to liquid fuels via pyrolysis: Review of commercial state-of-the-art and recent laboratory research, *Waste and Biomass Valorization*. 2 (2011) 227–255. doi:10.1007/s12649-011-9067-5.
- [28] G. Lopez, M. Artetxe, M. Amutio, J. Bilbao, M. Olazar, Thermochemical routes for the valorization of waste polyolefinic plastics to produce fuels and chemicals. A review, *Renew. Sustain. Energy Rev.* 73 (2017) 346–368. doi:10.1016/j.rser.2017.01.142.
- [29] M. Arabiourrutia, G. Elordi, G. Lopez, E. Borsella, J. Bilbao, M. Olazar, Characterization of the waxes obtained by the pyrolysis of polyolefin plastics in a conical spouted bed reactor, *J. Anal. Appl. Pyrolysis*. 94 (2012) 230–237. doi:10.1016/j.jaap.2011.12.012.
- [30] R. Sadeghbeigi, *Fluid catalytic cracking handbook*, 3rd ed., Butterworth Heinemann, 2012. doi:10.1017/CBO9781107415324.004.
- [31] A.T. Jarullah, I.M. Mujtaba, A.S. Wood, Kinetic parameter estimation and simulation of trickle-bed reactor for hydrodesulfurization of crude oil, *Chem. Eng. Sci.* 66 (2011) 859–871. doi:10.1016/j.ces.2010.11.016.
- [32] S. Al-Khattaf, The role of diffusion in alkyl-benzenes catalytic cracking, *Appl. Catal. A Gen.* 226 (2002) 139–153. doi:10.1016/S0926-860X(01)00895-X.
- [33] I.L.C. Buurmans, J. Ruiz-Martínez, W. V. Knowles, D. Van Der Beek, J. a. Bergwerff, E.T.C. Vogt, B.M. Weckhuysen, Catalytic activity in individual cracking catalyst particles imaged throughout different life stages by selective staining, *Nat. Chem.* 3 (2011) 862–867. doi:10.1038/nchem.1148.
- [34] P. Castaño, J. Ruiz-Martínez, E. Epelde, A.G. Gayubo, B.M. Weckhuysen, Spatial

- distribution of zeolite ZSM-5 within catalyst bodies affects selectivity and stability of methanol-to-hydrocarbons conversion, *ChemCatChem*. 5 (2013) 2827–2831. doi:10.1002/cctc.201300218.
- [35] U.J. Etim, B. Xu, P. Bai, R. Ullah, F. Subhan, Z. Yan, Role of nickel on vanadium poisoned FCC catalyst: A study of physiochemical properties, *J. Energy Chem.* 25 (2016) 667–676. doi:10.1016/j.jechem.2016.04.001.
- [36] H. Jiang, K.J. Livi, S. Kundu, W.C. Cheng, Characterization of iron contamination on equilibrium fluid catalytic cracking catalyst particles, *J. Catal.* 361 (2018) 126–134. doi:10.1016/j.jcat.2018.02.025.
- [37] M.A. den Hollander, M. Wissink, M. Makkee, J.A. Moulijn, Gasoline conversion: reactivity towards cracking with equilibrated FCC and ZSM-5 catalysts, *Appl. Catal. A Gen.* 223 (2002) 85–102. doi:10.1016/S0926-860X(01)00745-1.
- [38] A. Corma, P.J. Miguel, A.V. Orchillés, Product selectivity effects during cracking of alkanes at very short and longer times on stream, *Appl. Catal. A Gen.* 138 (1996) 57–73. doi:10.1016/0926-860X(95)00245-6.
- [39] Y. V Kissin, Chemical mechanisms of catalytic cracking over solid acidic catalysts: alkanes and alkenes, *Catal. Rev. - Sci. Eng.* 43 (2001) 85–146. doi:10.1081/CR-100104387.
- [40] B. Amblard, R. Singh, E. Gbordzoe, L. Raynal, CFD modeling of the coke combustion in an industrial FCC regenerator, *Chem. Eng. Sci.* 170 (2017) 731–742. doi:10.1016/j.ces.2016.12.055.
- [41] J.L. Fernandes, L.H. Domingues, C.I.C. Pinheiro, N.M.C. Oliveira, F.R. Ribeiro, Influence of different catalyst deactivation models in a validated simulator of an industrial UOP FCC unit with high-efficiency regenerator, *Fuel*. 97 (2012) 97–108. doi:10.1016/j.fuel.2012.03.009.
- [42] H.S. Cerqueira, C. Sievers, G. Joly, P. Magnoux, J.A. Lercher, Multitechnique characterization of coke produced during commercial resid FCC operation, *Ind. Eng. Chem. Res.* 44 (2005) 2069–2077. doi:10.1021/ie048963k.
- [43] H.S. Cerqueira, G. Caeiro, L. Costa, F. Ramôa Ribeiro, Deactivation of FCC catalysts, *J. Mol. Catal. A Chem.* 292 (2008) 1–13. doi:10.1016/j.molcata.2008.06.014.
- [44] A.I. Hussain, A. Palani, A.M. Aitani, J. Čejka, M. Shamzhy, M. Kubů, S.S. Al-Khattaf,

- Catalytic cracking of vacuum gasoil over -SVR, ITH, and MFI zeolites as FCC catalyst additives, *Fuel Process. Technol.* 161 (2017) 23–32. doi:10.1016/j.fuproc.2017.01.050.
- [45] T. Sonthisawate, T. Nakanishi, H. Nasu, T. Hashimoto, A. Ishihara, Catalytic cracking reaction of vacuum gas oil and atmospheric residue by zeolite-containing microporous and mesoporous composites using Curie point pyrolyzer, *Fuel Process. Technol.* 142 (2016) 337–344. doi:10.1016/j.fuproc.2015.10.016.
- [46] J. Fals, J.R. García, M. Falco, U. Sedran, Coke from SARA fractions in VGO. Impact on Y zeolite acidity and physical properties, *Fuel*. 225 (2018) 26–34. doi:10.1016/j.fuel.2018.02.180.
- [47] J. Alvira, I. Hita, E. Rodríguez, J. Arandes, P. Castaño, A data-driven reaction network for the fluid catalytic cracking of waste feeds, *Processes*. 6 (2018) 243. doi:10.3390/pr6120243.
- [48] H. De Lasa, Riser simulator, U.S. Patent. 5,102,628, 1992.
- [49] F.J. Passamonti, G.D. La Puente, U. Sedran, Comparison between MAT flow fixed bed and batch fluidized bed reactors in the evaluation of FCC catalysts. 1. Conversion and yields of the main hydrocarbon groups, *Energy Fuels*. 23 (2009) 1358–1363. doi:10.1021/ef8008103.
- [50] F.J. Passamonti, G.D. La Puente, U. Sedran, Comparison between MAT flow fixed bed and batch fluidized bed reactors in the evaluation of FCC catalysts. 2. Naphtha composition, *Energy Fuels*. 23 (2009) 3510–3516. doi:10.1021/ef900151e.
- [51] A. Alkhlel, H. de Lasa, Catalytic Cracking of Hydrocarbons in a CREC Riser Simulator Using a Y-Zeolite-Based Catalyst: Assessing the Catalyst/Oil Ratio Effect, *Ind. Eng. Chem. Res.* 57 (2018) 13627–13638. doi:10.1021/acs.iecr.8b02427.
- [52] I. Hita, M. Arabiourrutia, M. Olazar, J. Bilbao, J.M. Arandes, P. Castaño, Opportunities and barriers for producing high quality fuels from the pyrolysis of scrap tires, *Renew. Sustain. Energy Rev.* 56 (2016) 745–759. doi:10.1016/j.rser.2015.11.081.
- [53] P. Castaño, A. Gutiérrez, I. Villanueva, B. Pawelec, J. Bilbao, J.M. Arandes, Effect of the support acidity on the aromatic ring-opening of pyrolysis gasoline over Pt/HZSM-5 catalysts, *Catal. Today*. 143 (2009) 115–119. doi:10.1016/j.cattod.2008.10.029.
- [54] A. Gutiérrez, J.M. Arandes, P. Castaño, A.T. Aguayo, J. Bilbao, Role of acidity in the deactivation and steady hydroconversion of light cycle oil on noble metal supported

- catalysts, *Energy Fuels*. 25 (2011) 3389–3399. doi:10.1021/ef200523g.
- [55] S. Kalirai, P.P. Paalanen, J. Wang, F. Meirer, B.M. Weckhuysen, Visualizing dealumination of a single zeolite domain in a real-life catalytic cracking particle, *Angew. Chemie Int. Ed.* 55 (2016) 11134–11138. doi:10.1002/anie.201605215.
- [56] E.T.C. Vogt, B.M. Weckhuysen, Fluid catalytic cracking: recent developments on the grand old lady of zeolite catalysis, *Chem. Soc. Rev.* 44 (2015) 7342–7370. doi:10.1039/C5CS00376H.
- [57] P. Magnoux, H. S. Cerqueira, M. Guisnet, Evolution of coke composition during ageing under nitrogen, *Appl. Catal. A Gen.* 235 (2002) 93–99. doi:10.1016/S0926-860X(02)00242-9.
- [58] A. Ochoa, A. Ibarra, J. Bilbao, J.M. Arandes, P. Castaño, Assessment of thermogravimetric methods for calculating coke combustion-regeneration kinetics of deactivated catalyst, *Chem. Eng. Sci.* 171 (2017) 459–470. doi:10.1016/j.ces.2017.05.039.
- [59] A. Ochoa, B. Valle, D.E. Resasco, J. Bilbao, A.G. Gayubo, P. Castaño, Temperature programmed oxidation coupled with in situ techniques reveal the nature and location of coke deposited on a Ni/La₂O₃-(α)Al₂O₃ catalyst in the steam reforming of bio-oil, *ChemCatChem*. 10 (2018) 2311–2321. doi:10.1002/cctc.201701942.
- [60] F. Bauer, H.G. Karge, Characterization of coke on zeolites, *Mol. Sieves*. 5 (2007) 249–364. doi:10.1007/3829_005.
- [61] G. Jiménez-García, H. de Lasa, R. Quintana-Solórzano, R. Maya-Yescas, Catalyst activity decay due to pore blockage during catalytic cracking of hydrocarbons, *Fuel*. 110 (2013) 89–98. doi:10.1016/j.fuel.2012.10.082.
- [62] G. Elordi, M. Olazar, G. Lopez, P. Castaño, J. Bilbao, Role of pore structure in the deactivation of zeolites (HZSM-5, H β and HY) by coke in the pyrolysis of polyethylene in a conical spouted bed reactor, *Appl. Catal. B Environ.* 102 (2011) 224–231. doi:10.1016/j.apcatb.2010.12.002.
- [63] A.T. Aguayo, P. Castaño, D. Mier, A.G. Gayubo, M. Olazar, J. Bilbao, Effect of cofeeding butane with methanol on the deactivation by coke of a HZSM-5 zeolite catalyst, *Ind. Eng. Chem. Res.* 50 (2011) 9980–9988. doi:10.1021/ie200946n.
- [64] P. Castaño, G. Elordi, M. Olazar, J. Bilbao, Imaging the profiles of deactivating species

- on the catalyst used for the cracking of waste polyethylene by combined microscopies, *ChemCatChem*. 4 (2012) 631–635. doi:10.1002/cctc.201100506.
- [65] Á. Ibarra, A. Veloso, J. Bilbao, J.M.M. Arandes, P. Castaño, A. Ibarra, A. Veloso, J. Bilbao, J.M.M. Arandes, P. Castaño, Dual coke deactivation pathways during the catalytic cracking of raw bio-oil and vacuum gasoil in FCC conditions, *Appl. Catal. B Environ.* 182 (2016) 336–346. doi:10.1016/j.apcatb.2015.09.044.
- [66] H. Zhang, S. Shao, R. Xiao, D. Shen, J. Zeng, Characterization of coke deposition in the catalytic fast pyrolysis of biomass derivatives, *Energy Fuels*. 28 (2014) 52–57. doi:10.1021/ef401458y.
- [67] S. Shao, H. Zhang, R. Xiao, X. Li, Y. Cai, Evolution of coke in the catalytic conversion of biomass-derivates by combined in-situ DRIFTS and ex-situ approach: Effect of functional structure, *Fuel Process. Technol.* 178 (2018) 88–97. doi:10.1016/J.FUPROC.2018.05.021.
- [68] S. Shao, H. Zhang, R. Xiao, X. Li, Y. Cai, Catalytic conversion of biomass-derivates by in situ DRIFTS: Evolution of coke, *J. Anal. Appl. Pyrolysis*. 127 (2017) 258–268. doi:10.1016/J.JAAP.2017.07.026.
- [69] H. Zhang, Y. Wang, S. Shao, R. Xiao, An experimental and kinetic modeling study including coke formation for catalytic pyrolysis of furfural, *Combust. Flame*. 173 (2016) 258–265. doi:10.1016/J.COMBUSTFLAME.2016.08.019.
- [70] H. Zhang, Y.-T. Cheng, T.P. Vispute, R. Xiao, G.W. Huber, Catalytic conversion of biomass-derived feedstocks into olefins and aromatics with ZSM-5: the hydrogen to carbon effective ratio, *Energy Environ. Sci.* 4 (2011) 2297. doi:10.1039/c1ee01230d.
- [71] A.T. Aguayo, A.G. Gayubo, J. Ereña, A. Atutxa, J. Bilbao, Coke aging and its incidence on catalyst regeneration, *Ind. Eng. Chem. Res.* 42 (2003) 3914–3921. doi:10.1021/ie030085n.
- [72] A.C. Ferrari, J. Robertson, Interpretation of Raman spectra of disordered and amorphous carbon, *Phys. Rev. B*. 61 (2000) 14095–14107. doi:10.1103/PhysRevB.61.14095.
- [73] A.C. Ferrari, Raman spectroscopy of graphene and graphite: Disorder, electron-phonon coupling, doping and nonadiabatic effects, *Solid State Commun.* 143 (2007) 47–57. doi:10.1016/j.ssc.2007.03.052.
- [74] B. Guichard, M. Roy-Auberger, E. Devers, B. Rebours, A.A. Quoineaud, M. Digne,

- Characterization of aged hydrotreating catalysts. Part I: Coke depositions, study on the chemical nature and environment, *Appl. Catal. A Gen.* 367 (2009) 1–8. doi:10.1016/j.apcata.2009.07.024.
- [75] M. Ibáñez, B. Valle, J. Bilbao, A.G. Gayubo, P. Castaño, Effect of operating conditions on the coke nature and HZSM-5 catalysts deactivation in the transformation of crude bio-oil into hydrocarbons, *Catal. Today.* 195 (2012) 106–113. doi:10.1016/j.cattod.2012.04.030.
- [76] T. Cordero-Lanzac, I. Hita, A. Veloso, J.M. Arandes, J. Rodríguez-Mirasol, J. Bilbao, T. Cordero, P. Castaño, Characterization and controlled combustion of carbonaceous deactivating species deposited on an activated carbon-based catalyst, *Chem. Eng. J.* 327 (2017) 454–464. doi:10.1016/j.cej.2017.06.077.
- [77] N. Chaouati, A. Soualah, M. Chater, M. Tarighi, L. Pinard, Mechanisms of coke growth on mordenite zeolite, *J. Catal.* 344 (2016) 354–364. doi:10.1016/J.JCAT.2016.10.011.
- [78] S. Müller, Y. Liu, M. Vishnuvarthan, X. Sun, A.C. Van Veen, G.L. Haller, M. Sanchez-Sanchez, J.A. Lercher, Coke formation and deactivation pathways on H-ZSM-5 in the conversion of methanol to olefins, *J. Catal.* 325 (2015) 48–59. doi:10.1016/j.jcat.2015.02.013.